Figure S1: Unique GL261 glioma-induced changes in the thymus are distinct from those induced by stress. (A) Methylene blue staining of RNA isolated from thymi. 28S, 18S ribosomal RNAs and samples selected for RNAseq analysis are indicated. (B and C) Differential gene expression in thymi of GL261-bearing compared to sham (PBS-injected) mice (B) and sham to naïve controls (C). Volcano plots show significance ($-\log_{10}$ p-values) against $\log_2$ differences in gene expression between the samples as determined by ANOVA and post t test. Colors indicate those genes found significantly up-regulated at least 2-fold (green), down-regulated at least 2-fold (red) or significantly up- or down-regulated less than 2-fold (yellow) in GL261 compared to naïve conditions (see main Figure 3C). (D and E) Expression levels of thymic epithelial cell genes *Epcam* and *Aire* (D) and T cell-specific genes *Thy1* and *Rag2* (E) in thymi from PBS-injected, GL261-bearing, and naïve mice, expressed as $\log_2$-transformed gene-specific reads per million total reads. Symbols indicate individual samples (n=3), black bar indicates mean +/- standard deviation. Statistical analysis was performed using a two-way ANOVA with multiple comparison test. *, $p<0.05$; **, $p<0.01$; ***, $p<0.001$, ns, no statistically significant difference between groups. (F-H) Flow cytometry of enzymatically digested naïve and glioma-bearing thymi are shown. In this experiment, samples were analyzed on a Cytek Aurora cytometer. (F) Total cell counts of CD45- cells, (G) CD45- Epcam+ cells, and (H) CD45- Epcam+ $MHCII^{hi}$ cells in the thymus are not significantly different between GL261-bearing and naïve mice (n=11 for naïve, and n=8 for GL261-tumor-beaing). In F-H thymi are harvested at the time GL261-beaing mice become moribund. Naïve mice were time-matched and age-matched and individually harvested at the time tumor-bearing mice became moribund. For gating, following selection of single cells and live cells, we excluded CD45+ cells and quantified CD45- cells. Within the CD45- population, we gated on Epcam+ epithelial cells, and MHCII expression was further quantified on this population. Mann-Whitney U test was used for assessing statistical significance (Ns, $p \geq 0.05$). (I) Acute phase response pathway is amongst top highly enriched pathways in our data set according to IPA. (J) IPA analysis of highly differentially expressed genes. Shown are the most significantly affected pathways. Positive z-scores (orange bars) indicate up-regulated pathways; negative z-scores indicate down-regulated pathways.

Figure S1: Unique GL261 glioma-induced changes in the thymus are distinct from those induced by stress.

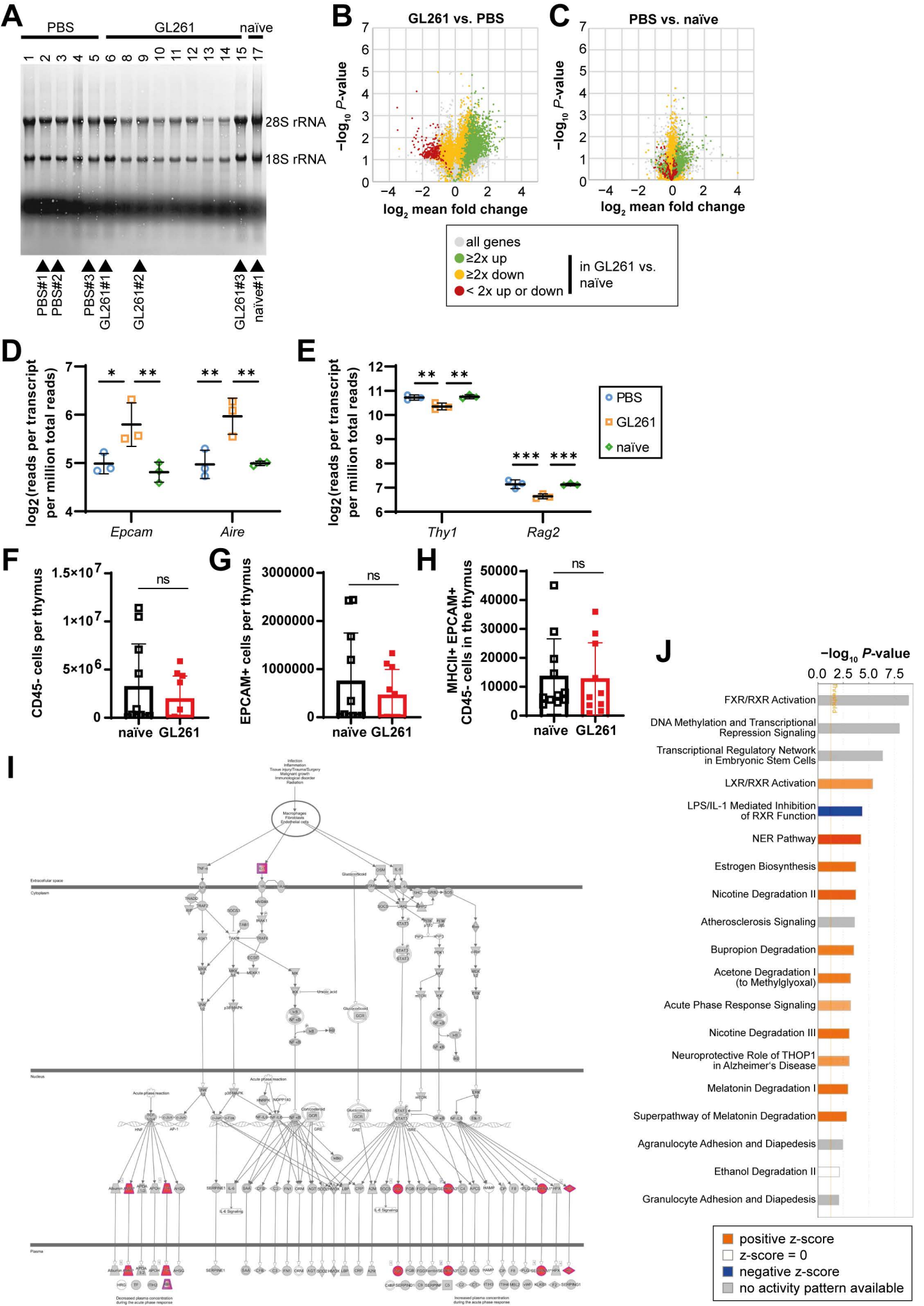

Figure S2: A sustained and continuous decline in T-cells is a hallmark feature of a growing glioma in the brain: (A) Tumor burden is tracked in representative mice shown in Figure 4 A-B in. # represents the day mouse succumb to death (14 and 21 for the representative mice shown). (B) Frequencies of CD4 and (C) CD8 are shown in mice implanted with GL261 cells. (D) Frequencies of CD4, and CD8 and (E left) B-cells are shown as a frequency of live cells in blood. (E right) Counts of $B220^+$ cells are shown per 100µl of blood. For T-cell gating, we gated on singlets, live, $CD45^+$ $TCR\beta^+$ B220- cells and then gated on either CD4 or CD8 T-cells. For B220 gating, we used a similar gate and instead focused non $TCR\beta^+$ cells that stained positive for B220. (F) Frequencies of CD4, CD8 and (G left) $B220^+$ cells are shown as a fraction of live cells per spleen. (G right) Counts of $B220^+$ and (H) $CD45^+$ leukocytes are shown. (D-H) data is collected when GL261 glioma-bearing mice become moribund. Individual naïve mice were euthanized when GL261-glioma-bearing mice became moribund. (I) Survival of glioma-bearing $MHCII^{-/-}$ and WT mice is compared within one experiment (n= 4 for WT and n=3 for $MHCII^{-/-}$). (J) Survival of WT (n=42 pooled from 3-4 independent experiments) and $MHCII^{-/-}$ (n=7 pooled from 2 independent experiments) mice implanted with GL261-Luc cells are compared. For survival data Log-rank (Mantel-Cox) test was used (in (J), MST WT =30 days vs. 24 days for $MHCII^{-/-}$). One way Anova with Tukey's multiple comparisons (when comparing more than two groups) test or a Mann-Whitney U test was used to calculate statistical significance (when comparing two groups) was used to assess statistical significance. Ns $p \geq 0.05$, * p= 0.01 to 0.05, ** p=0.001 to 0.01, ***p=0.0001 to 0.001, **** p< 0.0001.

Figure S2: A sustained and continuous decline in blood T cells is a hallmark feature of a growing glioma in the brain

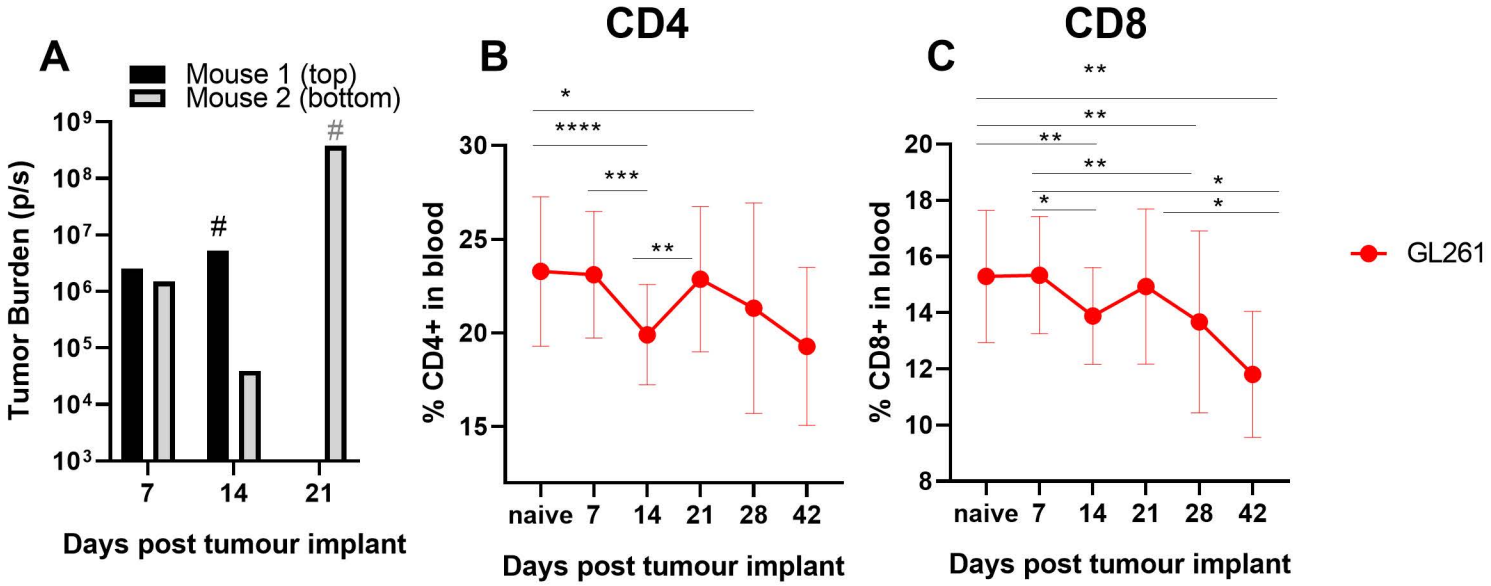

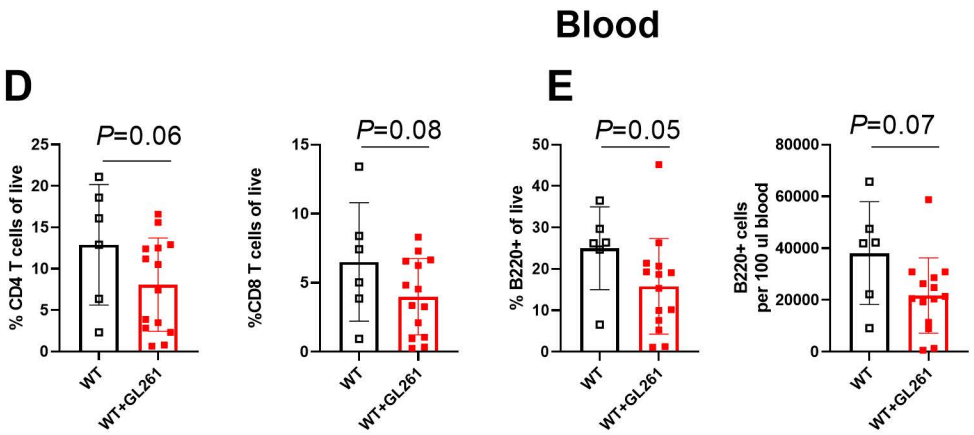

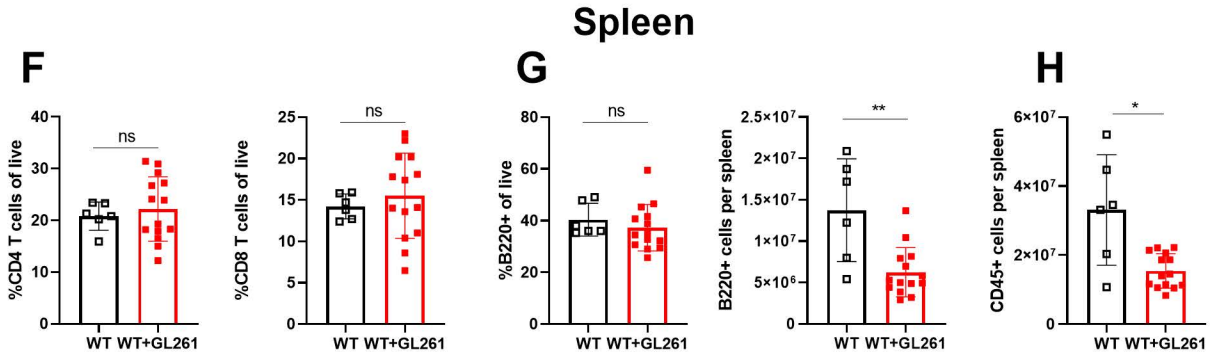

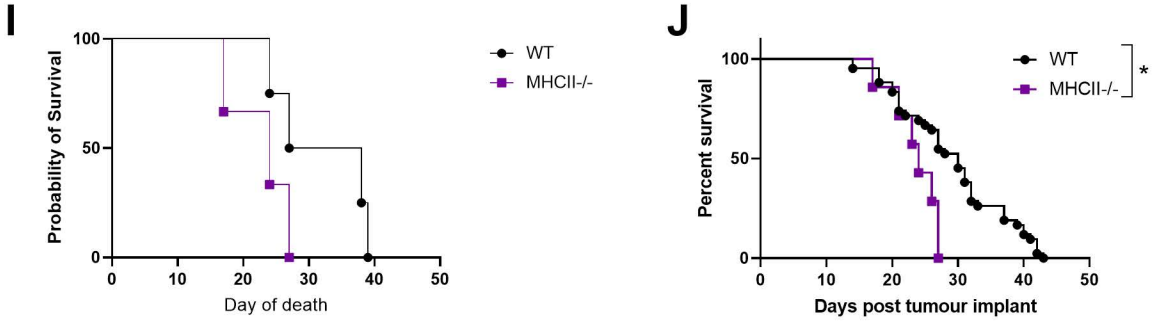

Figure S3: CD4 T-cells preferentially accumulate in the bone marrow of glioma-bearing mice

(A) A modest number of T-cells accumulate in the bone marrow of glioma-bearing mice when compared to naïve controls. (B) Frequency (left) and absolute numbers of T-cells (right) in the bone marrow of GL261-glioma-beaing and naïve controls are shown. (C) The increase in the bone marrow T-cells is mainly due to an increase in frequencies and numbers of CD4 T-cells. (D) The increase in bone marrow resident CD8 T-cells in glioma-bearing mice does not reach statistical significance. (E) Representative flow plot of CD4 T-cells within the bone marrow indicates CD4 T-cells with $CD62L^{hi}$ $CD69^{-}$ phenotype to accumulate in glioma-bearing mice compared to controls. (F) Frequencies and absolute counts of $CD62L^{hi}$ $CD69^{-}$ CD4 T-cells are quantified in naïve and glioma-bearing mice. (G) Total cellularity of bone marrow does not change between naïve and glioma-bearing mice. Similarly, (H) frequencies and numbers of B-cells and (I) CD11b+ cells in the bone marrow does not change between naïve and glioma-bearing mice. (A-I) Bone marrow was assessed at the time GL261-glioma-bearing mice became moribund. Individual naïve control mice were euthanized at the time GL261-glioma-bearing mice were moribund. GL261+ group represents mice that were intracranially implanted with the glioma cell lines (GL261-Luc) and were verified to be tumor-bearing by bioluminescence imaging. Data is presented is at the time GL261+ mice became moribund. Naïve controls are sex/age matched. Bone marrow was isolated from two femurs from each animal. For gating, we used a strategy that included gates for single cells, live cells, CD45+ cells, TCRβ+ cells, before gating for CD4 and/or CD8 T-cells. Within the CD4 gated population, we then used CD62L and CD69 to further investigate the phenotype of bone marrow resident T-cells. Data is shown from 6 naïve controls and 14 GL261-glioma-bearing mice. Individual data points are shown. Error bars represent standard deviation. Mann-Whitney U test was used to assess statistical significance. Ns $p \geq 0.05$, * p= 0.01 to 0.05, ** p=0.001 to 0.01, ***p=0.0001 to 0.001, **** p< 0.0001.

Figure S3: CD4 T cells preferentially accumulate in the bone marrow of glioma-bearing mice

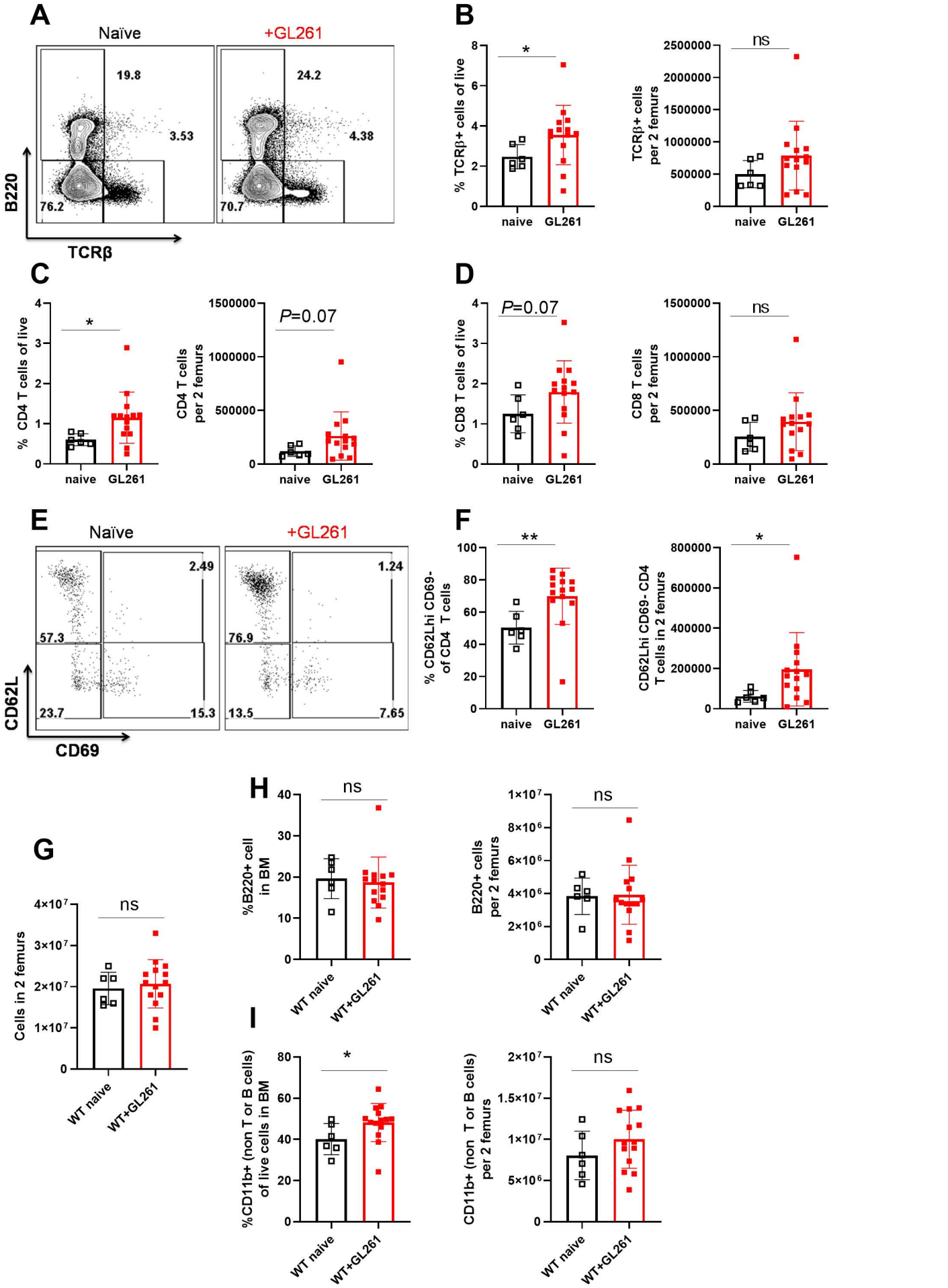

Figure S4: Immunosuppression during experimental-GBM is transferrable to naïve mice via blood circulation: (A) Tumor burden is shown in tumor-bearing parabiont and tumor-negativity is confirmed in naïve partner. Values below 10^5 are considered tumor-negative. (B) Survival of 3-parabiotic pairs was within the range of WT mice (n=43, pooled from several experiments as presented in Figure 1 and S2. This serves as historical control). (C) Frequencies of CD4, (D) CD8, and (E) expression levels of MHCII are shown in all mice following analysis of the blood by flow cytometry. (F) Frequencies of GFP^+ cells were maintained within all 6 mice throughout the experiment.

Figure S4: Immunosuppression during experimental-GBM is transferrable to naïve mice via blood circulation

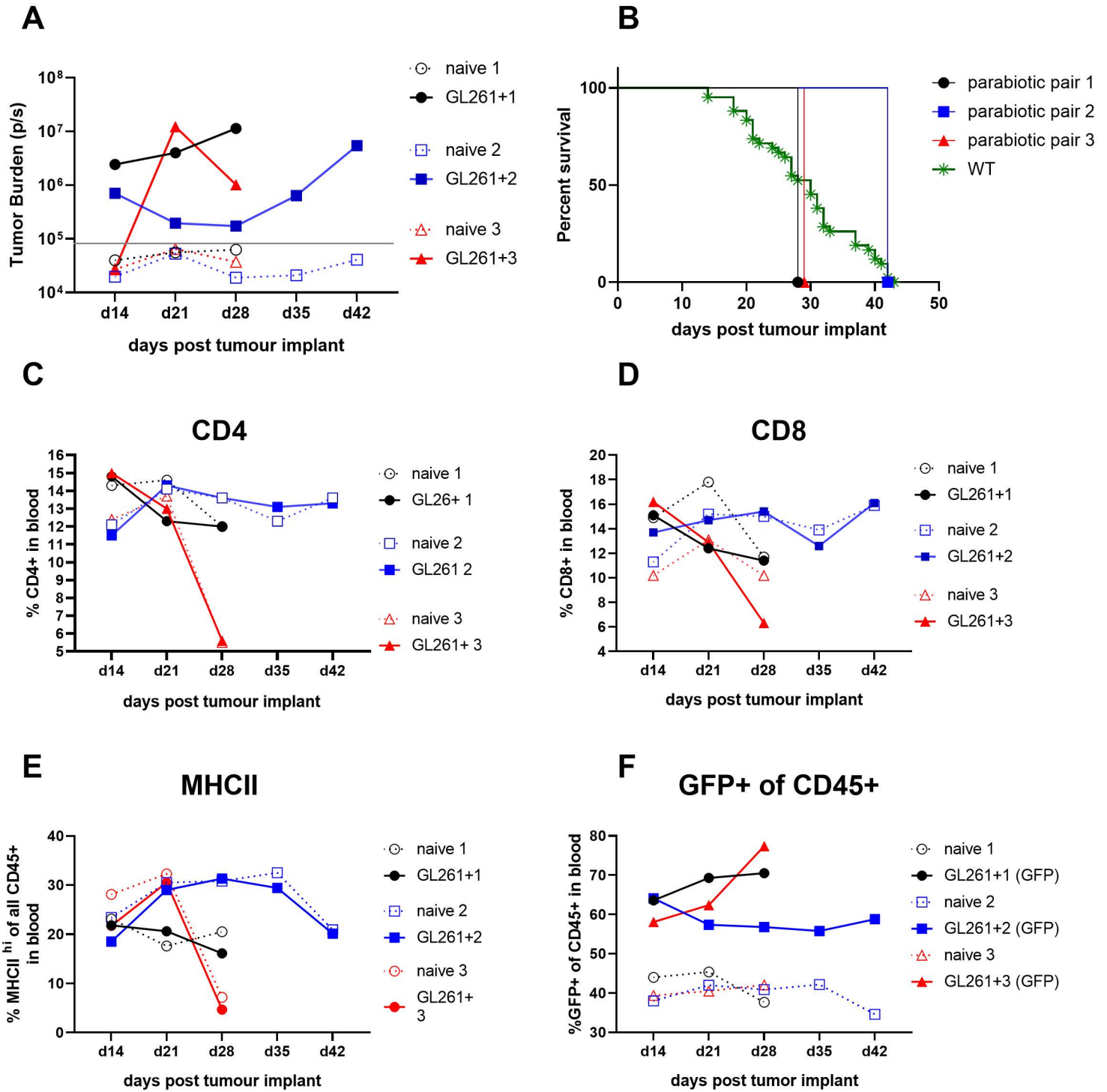

Figure S5: Hallmark features of immunosuppression do not occur following parabiosis of naïve-to-naïve mice: we performed parabiosis on 6 pairs of naïve mice. In each parabiotic pair, one mouse was GFP^{+}. 30 days later, we implanted GL261-Luc cells in the brains of 3 mice. Naïve-to-tumor-bearing parabionts were euthanized when tumor-bearing mice became moribund. Naïve-to-naïve parabiont controls were euthanized on day 60 post parabiosis. (A) Thymic cellularity (B) and thymic weight in glioma-bearing and tumor-free parabionts is compared to naïve age-matched historical controls. (C) Naïve-to-naïve parabiotic mice had stable sharing of GFP+ cells. (D) CD4, CD8 T-cells, and (E) MHCII expression on all CD45+ cells in the blood do not decline in naïve-naïve pairs on day 60 post parabiosis.

Figure S5: Hallmark features of immunosuppression do not occur following parabiosis of naïve-to-naïve mice

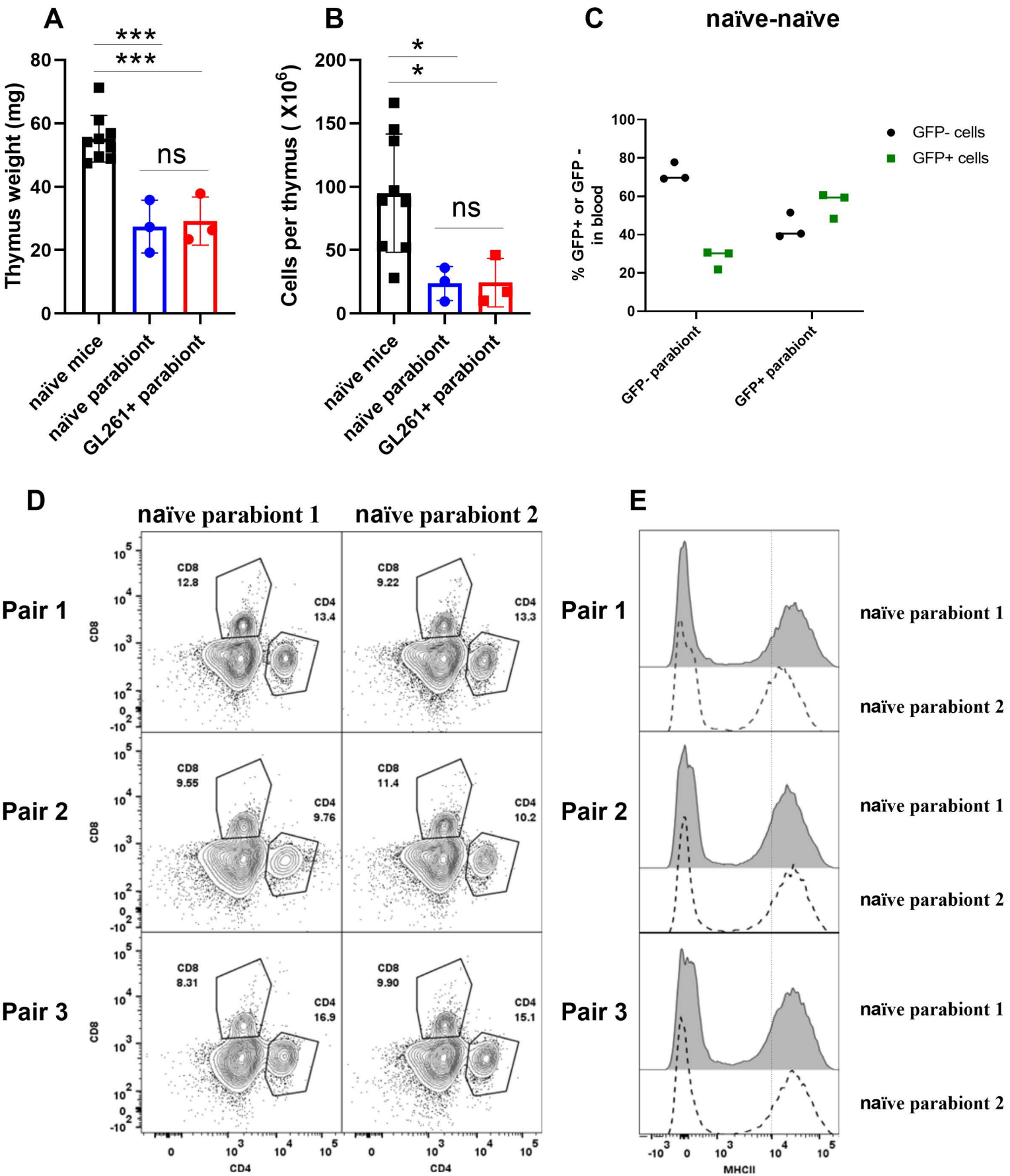

Figure S6: Seizure activity correlates with thymic involution on day 7 post KA injection: (A) Individual seizure scores are shown for male and (C) female mice as a function of time post KA injection. (B) Thymic cellularity for male mice is quantified. # denotes one mouse that did not have a seizure despite KA injection. (B) This mouse did not develop thymic involution on day 7 post KA injections. (D) Thymic cellularity in female mice is quantified. These experiments were done in male mice and repeated in female mice in an independent experiment. N=4-8.

Figure S6: Seizure activity correlates with thymic involution on day 7 post KA injection:

A

Male mice

Mouse number	1	2	3	4	5	6	7	8	9	10
5min	1	1	1	1	0 #	1	1	1	1	1
10min	5	1	1	1	0	1	1	4	1	2
15min	5	2	2	2	0	1	1	5	2	2
20min	7	2	2	7	0	1	1	7	2	2
25min		2	2		0	1	1		2	5
30min		1	2		0	1	1		1	5
35min		1	4		0	1	1		1	5
40min		1	4		0	1	1		1	5
45min		1	5		0	1	1		1	4
50min		1	4		0	1	1		1	4
55min		1	4;stop		0	1	1		1	4; stop
60min		3			0	2	1		1	
65min		2			0	2	1		2	7
70min		stop			0	2	1		2	
75min					0	2	0		2	
80min			7		0	1	0		stop	
85min					0	1	0			
90min					0	2	1			
95min					0	stop	stop			
100min					0					
105min					0					
110min					0					
115min					0					
120min					stop					

B

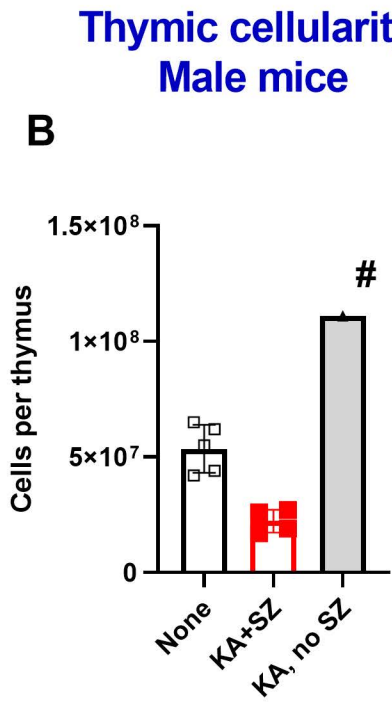

C

Female mice

Mouse number	1	2	3	9	10	11	12	13
5min	0	1	1	0	1	1	1	1
10min	0	1	1	0	1	1	1	1
15min	0	1	1	0	2	2	1	2
20min	0	1	2	0	2	2	0	0
25min	0	1	1	0	1	1	1	0
30min	0	1	1	0	2	1	1	0
35min	0	1	1	1	1	1	0	1
40min	0	1	1	1	2	1	0	0
45min	0	1	0	1	0	1	0	0
50min	0	1	1	tail shake	1	0	tail shake	0
55min	inject nothing	inject 3mg/kg	inject 3mg/kg	inject 3mg/kg	inject 3mg/kg	inject 3mg/kg	inject 3mg/kg	inject 3mg/kg
60min	0	1	1	1	1	1	0	1
65min	0	1	1	1	1	0	1	1
70min	0	1	1	1	1	1	1	0
75min	0	1	1	1	1	1	1	1
80min	1	1	1	tail shake	1	1	tail shake	1
85min	0	1	1	1	1	1	1	1
90min	stop	stop	stop	stop	stop	stop	stop	stop

D

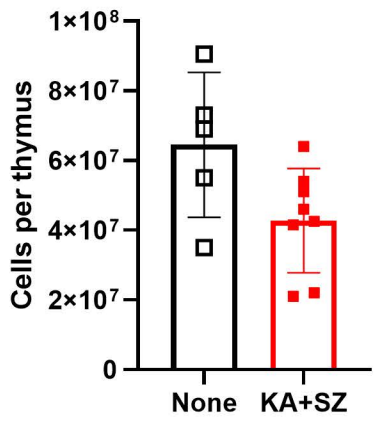

Figure S7: Serum obtained from mice with an ongoing neurological insult suppresses T-cell proliferation *in vitro*: (A) Representative histograms depict CD4 (top) and CD8 (bottom) T-cell proliferation with anti-CD3/CD28 Dynabeads. Serum isolated from mice injected with B16 melanoma (i.c) is tested for suppressive activity against T-cells. (B-C) Quantification of T-cell proliferation following exposure to serum obtained from naïve or TMEV infected mice (day 7 post intracranial infection) is shown for CD4 and CD8 T-cells. (D) Serum obtained from PBS (i.c) injected mice on days 7, 11 and 21 post injection is tested for suppressive activity against T-cells. These experiments were repeated twice with similar results. Representative histograms are shown.

Figure S7: Serum obtained from mice with an ongoing neurological insult suppresses T cell proliferation *in vitro*

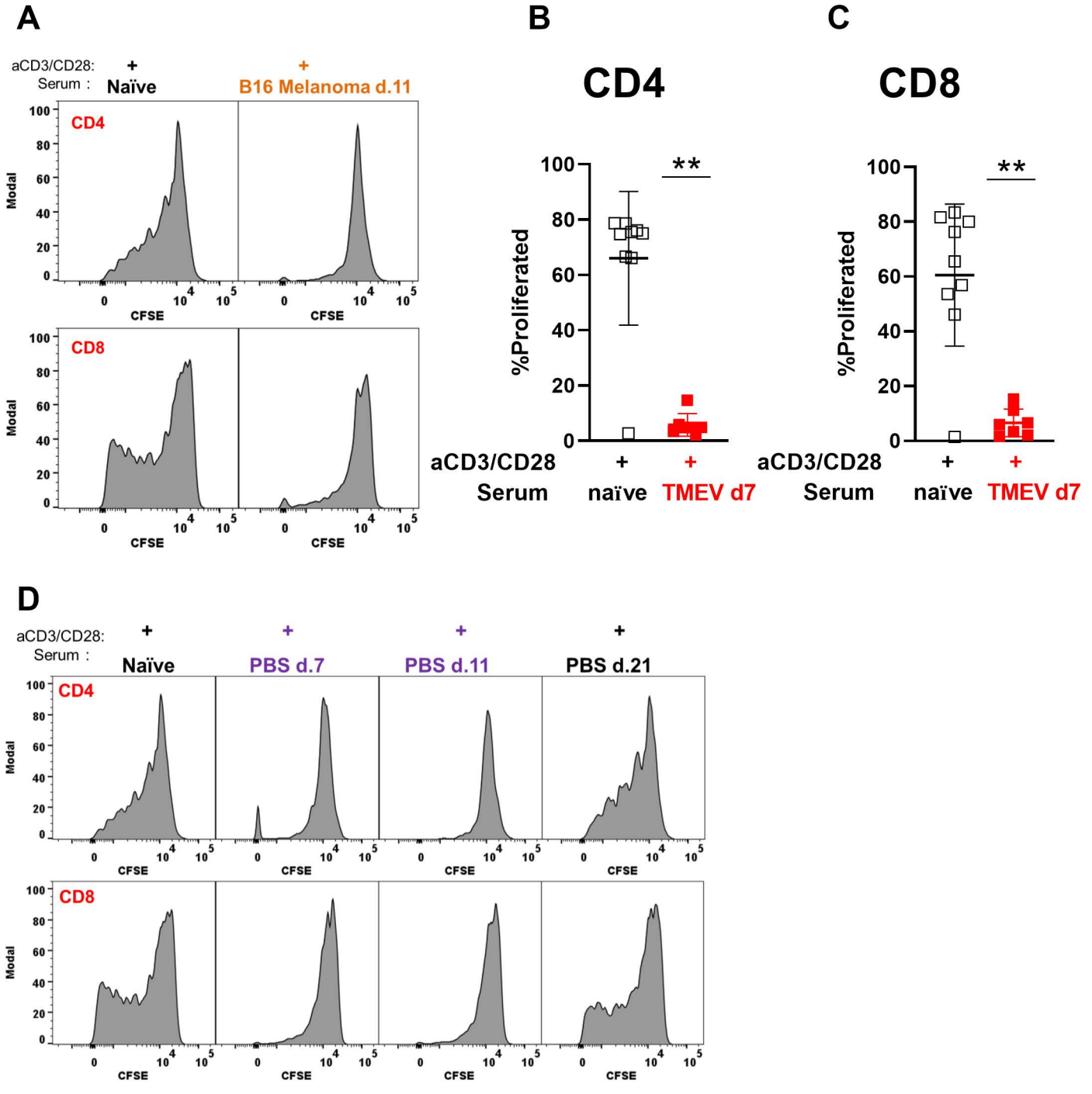

Figure S8: Hormones produced by the adrenal gland control immune organ size and cellularity at baseline: (A) Frequencies of CD4, (B) CD8, (C) B220 cells are compared in blood of naïve WT and adrenalectomized mice. (D-E) Frequencies of CD4 and CD8 T-cells in the blood do not change between naïve and glioma-bearing adrenalectomized mice. (F) Numbers of B-cells in 100µl of blood do not change in glioma-bearing mice compared to naïve adrenalectomized controls. (G-H) Frequencies and numbers of $MHCII^{hi}$ B-cells decline in blood of glioma-bearing WT mice compared to WT controls, but do not change amongst adrenalectomized counterparts. (I) Numbers of B-cells, and (J) numbers of $MHCII^{hi}$ B-cells are compared in spleens of WT and Adrenalectomized mice. (K) Frequencies of DN1-DN4, (L) DP, and (M) single positive CD4 and CD8 T-cells are shown for thymi isolated from naïve and glioma-bearing WT and adrenalectomized mice. One way Anova with Tukey's multiple comparisons test (when comparing more than two groups) or a Mann-Whitney U test was used to calculate statistical significance (when comparing two groups) significance. Ns $p \geq 0.05$, * p= 0.01 to 0.05, ** p=0.001 to 0.01, ***p=0.0001 to 0.001, **** p< 0.0001.

Figure S8: Hormones produced by the adrenal gland control immune organ size and cellularity at baseline

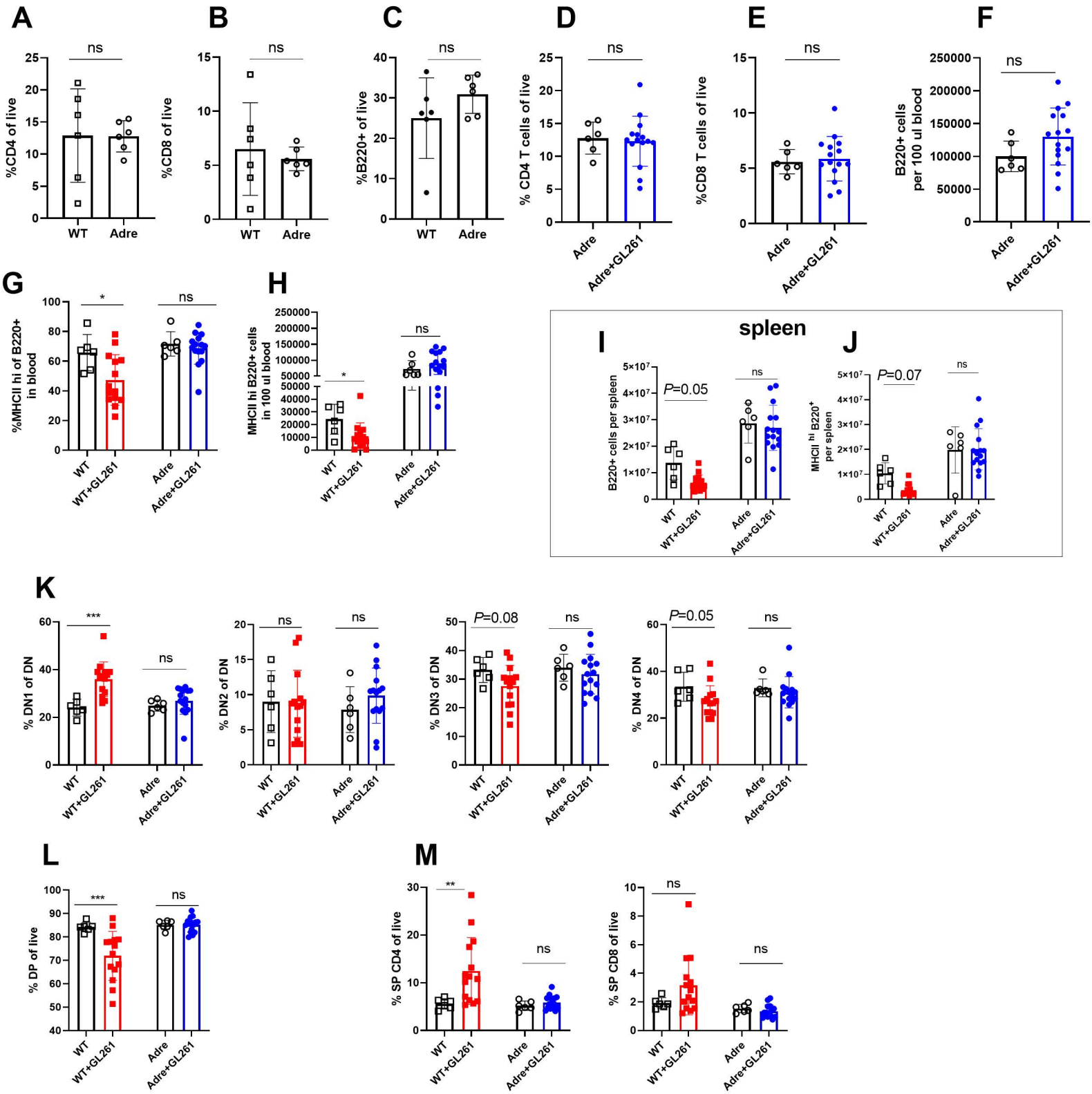

Supplementary Table 1

Adrenalectomized mice only had the serum-derived immunosuppressive factor aspect of immunosuppression and did not have other facets of immunosuppression (including thymic and spleen involution, T-cell reduction in blood, T-cell accumulation in the bone marrow, or MHCII downregulation). However, these data suggest that the immunosuppressive serum-derived factor alone is sufficient to prevent a survival benefit.

	Thymic involution (thymus)	Spleen atrophy (spleen)	Decrease in T cell counts (blood)	MHCII down-regulation (blood, spleen)	T cell sequestration in the BM (BM)	Presence of a non-steroid large immunosuppressive/ anti proliferative factor in serum	MST (GL261-Luc)
WT	Yes	Yes	Yes	Yes	Yes	Yes	27 days
Adre	No	No	No	No	No	Yes	23 days